

# Geochemical and Sr–Nd–Pb isotopic compositions of Cretaceous granitoids: constraints on tectonic framework and crustal structure of the Dabieshan ultrahigh-pressure metamorphic belt, China

Hongfei Zhang<sup>a,\*</sup>, Shan Gao<sup>a,b</sup>, Zengqiu Zhong<sup>a</sup>, Benren Zhang<sup>a</sup>,  
Li Zhang<sup>a</sup>, Shenhong Hu<sup>a</sup>

<sup>a</sup>*Faculty of Earth Sciences, China University of Geosciences, Wuhan 430074, PR China*

<sup>b</sup>*Department of Geology, Northwest University, Xi'an 710069, PR China*

## Abstract

The Dabie orogenic belt can be divided into four tectonic and lithological units. They are, from north to south, the North Huaiyang (NHY) unit, the Northern Dabie complex (NDC) unit, the ultrahigh-pressure (UHP) metamorphic unit, and high-pressure (HP) metamorphic unit. Cretaceous granitoids from the four tectonic units, irrespective of tectonic unit and lithology, show surprisingly similar major and trace element and particularly Sr–Nd–Pb isotopic compositions, indicating a similar crustal source for their magma genesis. They have initial ( $^{87}\text{Sr}/^{86}\text{Sr}$ )<sub>i</sub> values of 0.7068–0.7091 and Nd-depleted mantle model ages of 1.6–2.4 Ga and  $\epsilon_{\text{Nd}}(t)$  values at the time of their emplacement (120 Ma) ranging from –13 to –26. Their present-day Pb isotopic compositions are  $^{206}\text{Pb}/^{204}\text{Pb} = 15.62–17.06$ ,  $^{207}\text{Pb}/^{204}\text{Pb} = 15.21–15.44$ , and  $^{208}\text{Pb}/^{204}\text{Pb} = 36.59–37.81$ . With comparison to the Sr–Nd–Pb isotopic compositions of the basement rocks in the Dabie orogenic belt, the isotopic compositions of the Cretaceous granitoids indicate a source that is similar to the Northern Dabie complex but distinct from the ultrahigh-pressure metamorphic unit. This strongly suggests that the exposed Northern Dabie complex extends in the deep crust southward beneath the UHP/HP metamorphic units and northward beneath the North Huaiyang unit. The Northern Dabie complex is best interpreted as the core of a dome within the Dabie orogenic belt. The UHP/HP metamorphic unit is only a thin-skinned slab confined in shallower crustal levels over the Northern Dabie complex. Present tectonic framework for the UHP/HP terrain was formed by extensional tectonics and post the UHP/HP metamorphism. The Northern Dabie complex has an affinity to the Yangtze craton. The similar source for the Cretaceous granitoids also suggests that the suture between the North China and the Yangtze cratons is marked by the Xiaotian–Mozitang Fault separating the North Huaiyang unit and the Northern Dabie complex rather than the previously thought Wuhe–Shuiko Fault, which separates the Northern Dabie complex and the UHP unit. © 2002 Elsevier Science B.V. All rights reserved.

**Keywords:** Cretaceous granitoid; Tectonic framework; Crustal structure; Ultrahigh-pressure metamorphic belt; Dabieshan, China

## 1. Introduction

The Dabie–Sulu ultrahigh-pressure (UHP) metamorphic belt is the largest among seven recognized UHP belts in the world (Hacker et al., 1996) and is formed by collision between the North China and

\* Corresponding author. Fax: +86-27-87801763.

E-mail address: zhanghf@public.wh.hb.cn (H. Zhang).

Yangtze cratons (Ames et al., 1993). Here, continental crust was deeply subducted and then rapidly exhumed from mantle depths back to crustal levels (Ye et al., 2000). It is unique in the abundance and variety of the UHP rocks exposed, and since the discovery of coesite-bearing eclogites (Xu, 1987; Okay et al., 1989; Wang et al., 1989) and diamond-bearing eclogites (Xu et al., 1992), it has become an outstanding geological location for studying ultrahigh-pressure metamorphism. Although numerous geological and geochronological studies have been made on the Dabie–Sulu region, the tectonic relation between the UHP metamorphic unit and the Northern Dabie complex is still a matter of great controversy. There are two contrasting views. The first considers that the UHP metamorphic block is underlying the Northern Dabie complex and that the contact between the UHP metamorphic unit and the Northern Dabie complex unit, which is marked by the Wuhe–Shuiko Fault, represents the suture between the Yangtze and North China cratons (Cong et al., 1996, 1999; Wang and Cong, 1996; Zhai and Cong, 1996). However, recent tectonic studies indicate that the UHP unit is a rootless slab overlying the Northern Dabie complex unit (Faure et al., 1999; Suo et al., 1999, 2000). Deep seismic refraction profiling also shows that the UHP rocks are confined to less than 9 km in depth and the Northern Dabie complex extends beneath the UHP unit (Wang et al., 2000). This implies that the Wuhe–Shuiko Fault cannot be taken as the suture. Widespread U–Pb zircon ages of 700–800 Ma within the UHP metamorphic unit and the Northern Dabie complex unit lead Hacker et al. (1998) to speculate that the suture lies north of the Xiaotian–Mozitang Fault. A similar conclusion is also supported by tectonic studies (Hacker et al., 2000; Ratschbacher et al., 2000; Suo et al., 1999, 2000).

Granitoids, which are usually derived from middle to lower crustal depths, provide an alternative approach to probe the deep crustal composition and structure (Downes and Duthou, 1988; Farmer, 1992; Zhang et al., 1997). In the Dabieshan, postcollisional Cretaceous granitoids, ranging from 130 to 112 Ma in age (RGS-Anhui, 1987; Li and Wang, 1991; Zhou et al., 1992; Xu et al., 1994; Chen et al., 1995; Xie et al., 2001), are widely distributed in each tectonic unit. Petrological and geochemical data suggest that they are I-type granites (Xu et al., 1994; Li and Wang, 1991). Recent geochemical and isotopic studies show that the Creta-

ceous granitoids are products of crustal anatexis induced by basaltic underplating at the base of the crust (Ma et al., 1998). However, the detailed nature of their sources is unclear.

In this study, we present new geochemical and Sr–Nd–Pb isotopic data for the Cretaceous granitoids from each tectonic unit in the eastern Dabieshan. The data are used to trace the protolith nature of these granitoids and further test the previous thin-skinned UHP/HP slab tectonic model and suture location in the Dabieshan (Wang et al., 2000; Hacker et al., 2000; Ratschbacher et al., 2000; Suo et al., 1999, 2000).

## 2. Geological setting

The Dabieshan represents the eastern segment of the Qinling–Dabie orogenic belt between the North China and Yangtze cratons (Fig. 1). Tectonically, the Dabie orogenic belt can be divided, from north to south, into the North Huaiyang (NHY) unit, the Northern Dabie complex (NDC) unit, the ultrahigh-pressure (UHP) metamorphic unit, and the high-pressure (HP) metamorphic unit (Fig. 1).

(1) The North Huaiyang unit is bounded by the Xiaotian–Mozitang Fault in the south and is composed of the Foziling Group. The Foziling Group, which underwent only greenschist-facies metamorphism, consists of metapelite with intercalations of quartzite and marble. It is considered to be a Paleozoic sedimentary sequence deposited in a back-arc basin (Cong et al., 1996) or a fore-arc basin (Xu et al., 1994). This unit is considered to be the southern margin of the North China craton based on its Paleozoic sedimentary sequences, which are typical of the North China craton (Xu et al., 1994).

(2) The Northern Dabie complex (NDC) is bounded between the Xiaotian–Mozitang Fault in the north and the Wuhe–Shuihou Fault in the south. The NDC consists of orthogneiss with minor amphibolite, marble, mafic, and felsic granulites. In the orthogneiss, Hacker et al. (1998) reported U–Pb SHRIMP ages of 129–138 Ma in zircon rims and of 700–800 Ma in the zircon core. Xue et al. (1997) also reported two U–Pb zircon lower intercept ages of  $134 \pm 2.8$  and  $133.7 \pm 2.3$  Ma from the orthogneiss and a concordant U–Pb zircon age of  $756.6 \pm 0.8$  Ma from a mylonitic granite. It is considered that the 700–800 Ma ages represent the

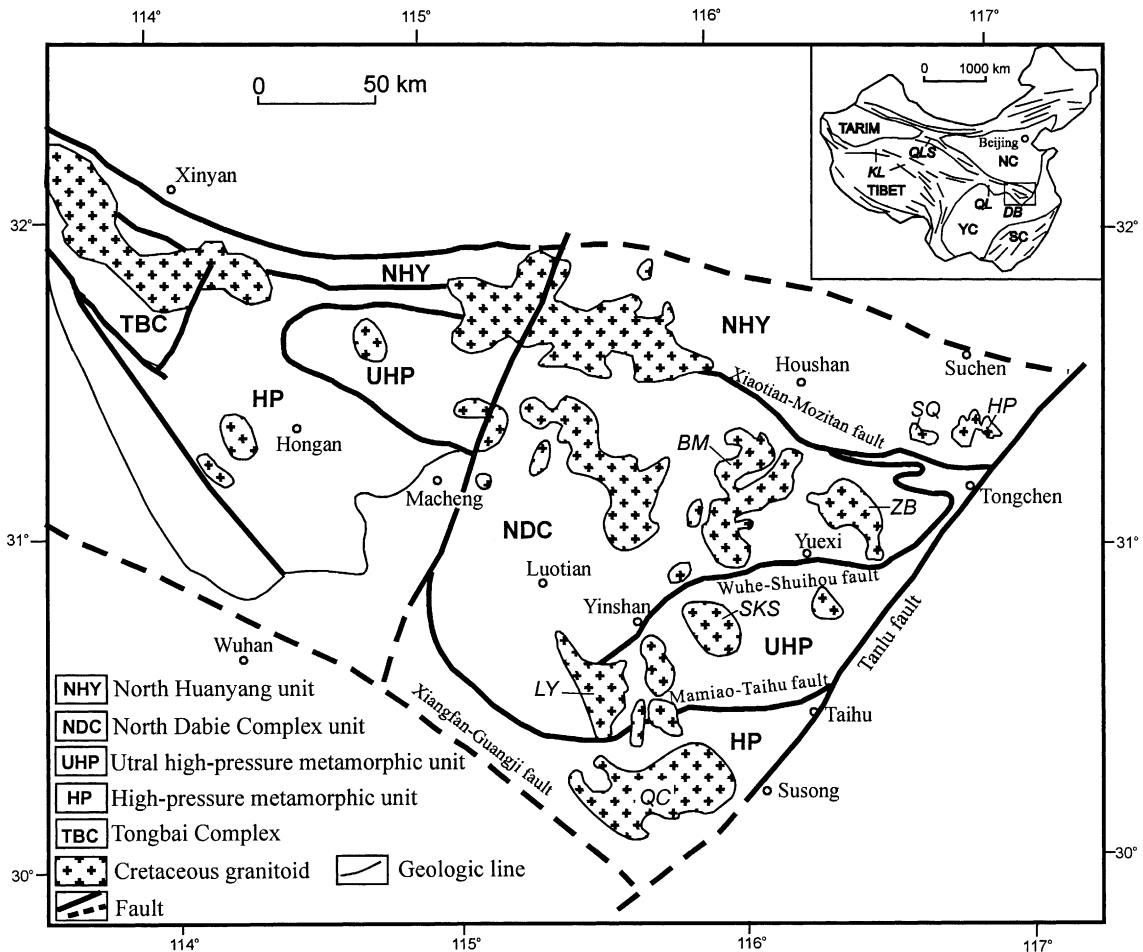


Fig. 1. Simplified geological map of Dabieshan. Inset shows location of study area. NC = North China craton; YC = Yangtze craton; SC = South China fold belt; KL = Kunlan Mountains; QLS = Qilian Mountains; QL = Qinling Mountains; DB = Dabieshan. Abbreviations of Cretaceous granitoid name: SQ = Shanqi; HP = Hepeng; BM = Baimajian; ZB = Zhubuyan; SKS = Sikongshan; LY = Luyan; QC = Qichuan.

ages of the orthogneiss protolith while the ages of 129–138 Ma represent timing of metamorphic overgrowth because the NDC was intruded by voluminous early Cretaceous undeformed granitoid plutons. Otherwise, it would be difficult to explain the short time interval between the formation of the foliated rocks (orthogneisses) and unfoliated Cretaceous granites. Although some Cretaceous plutons have undeformed cores and deformed margins (Hacker et al., 1998; Ratschbacher et al., 2000), detailed field geologic investigations show that these plutons display an intrusive contact with the NDC. Eclogites have recently been reported in the NDC by Wei et al. (1997), Xu et al. (1999), and Tsai and Liou (2000).

(3) The UHP metamorphic unit is bounded between the Wuhe–Shuihou Fault in the north and the Mamiao–Taihu Fault in the south. It consists mainly of gneiss with frequent and retrograded eclogites (garnet-bearing amphibolite), garnet-bearing peridotite, jadeite quartzite, and marble. This unit is characterized by occurrence of the UHP metamorphic rocks such as coesite-bearing eclogites (Okay et al., 1989, 1993; Wang et al., 1989; Cong et al., 1996; Xu et al., 1994) and rare microdiamond-bearing eclogites (Xu et al., 1992). The eclogites occur as lenses, boudins, blocks, or layers in gneisses, marble, and ultramafic rocks. Geochronological studies indicate that the UHP metamorphism occurred between 210 and 245 Ma (Hacker

et al., 1996, 1998; Li et al., 1993, 2000; Ames et al., 1996; Rowley et al., 1997; Chavagnac and Jahn, 1996). Sr–Nd isotopic tracer study suggests that the protolith of these eclogites are clearly of continental affinity (Jahn, 1998). The gneiss associated with the eclogites was considered to be mostly paragneiss (Cong et al., 1996; Wang and Liou, 1991), with the mineral assemblage quartz + bitotite + plagioclase  $\pm$  K-feldspar  $\pm$  garnet  $\pm$  phengite. Relict grossular + rutile assemblage, equigranular polygonal quartz aggregates in the matrix, and coesite pseudomorphs in garnet imply that the host gneiss of eclogites also underwent UHP metamorphism and thus form an in situ UHP slab (Wang and Liou, 1991; Liou et al., 1996, 1997).

(4) The HP metamorphic unit is bounded between the Mamiao–Taihu Fault in the north and the Xiangfan–Guangji Fault in the south. This unit is traditionally called the Susong Group (You et al., 1996), consisting of muscovite–albite gneiss and two-mica gneiss with minor eclogite, amphibolite, marble, metaphosphorite layer, and blueschist. The eclogites occur as lenses, boudins, blocks, or layers in the gneiss in the northern part of the belt. No coesite or its pseudomorph has been reported in the eclogites. Epidote-bearing blueschists are exposed in the southernmost part of

the belt near the Xiangfan–Guangji Fault. Thus, the metamorphic grade apparently decreases from north to south.

### 3. Cretaceous granitoids

Cretaceous granitoids are distinct from pre-Cretaceous granitoids in that the latter show strong foliation and tectonic deformation. The Cretaceous granitoid plutons are widely distributed in above four units (Fig. 1). They show sharp intrusive contact with the country rocks. Regional foliation is not developed within these plutons. The rock types for the Cretaceous granitoids range from quartz diorite to granodiorite to granite. Mafic enclaves rarely occur in the granodiorite and granite. The granitoids are medium-fine to coarse-grained with variable proportions of biotite and hornblende. Biotite is the most common mafic mineral. Detailed petrographic characteristics for the Cretaceous granitoids are described elsewhere (RGS-Anhui, 1987; Li and Wang, 1991; Xu et al., 1994; Ma et al., 1998).

Representative plutons from the four tectonic units are studied. Shanqi and Hepeng plutons are from the

Table 1  
Exposed area, rock type, and radiometric age of Dabieshan Cretaceous granitoid plutons

Pluton	Area (km <sup>2</sup> )	Rock type	Age (Ma)			
			U–Pb	Rb–Sr	Ar/Ar	Data source
<i>North Huaiyang unit</i>						
Shanqi (SQ)	20	quartz diorite				
Hepeng (HP)	80	biotite/hornblende monzogranite			124 ± 0.8 <sup>a</sup>	Zhou et al. (1992)
<i>Northern Dabie complex unit</i>						
Zhubuyan (ZB)	410	granodiorite; biotite/hornblende; monzogranite		118 ± 3		Xie et al. (2001)
Baimajian (BM)	580	biotite granite		112 ± 6		Xu et al. (1994)
<i>UHP unit</i>						
Sikongshan (SKS)	190	granodiorite granite			129 ± 0.5 <sup>a</sup> ; 126 ± 1.9 <sup>b</sup>	Chen et al. (1995)
Luyang (LY)	380	biotite monzogranite	112 ± 7 <sup>c</sup>			Li and Wang (1991)
<i>HP unit</i>						
Qichuan (QC)	760	granodiorite; hornblende monzogranite		121 ± 6	126 ± 0.7 <sup>a</sup> ; 116 ± 0.4 <sup>b</sup>	Chen et al. (1995) Li and Wang (1991)

<sup>a</sup> Hornblende.

<sup>b</sup> Biotite.

<sup>c</sup> Zircon.

NHY unit, the Zhuboyan and Baimajian plutons from the NDC unit, the Sikongshan and Luyang plutons from the UHP unit, and the Qichuan pluton from the HP unit. Area extent, rock type, and radiometric ages of the Cretaceous granitoid plutons under investigation are summarized in Table 1. Petrologically, the Shanqi (quartz diorite), the Hepeng (biotite/hornblende monzogranite), the Baimajian (biotite granite), the Luyang (biotite monzogranite), and the Sikongshan (granodiorite) plutons consist of only one rock type, while the Zhuboyan (granodiorite and biotite/hornblende monzogranite) and the Qichuan (granodiorite and hornblende-bearing monzogranite) plutons are composed of two rock types with the late phase being more evolved than the early phase. The contact between two rock types within a single pluton is intermingled, indicating that they were formed within a relatively short time interval. Mineralogically, the quartz diorites (e.g., the Shanqi) are composed of quartz (5–10%), plagioclase (40–55%), K-feldspar (2–5%), biotite (5–10%), and amphibole (20–30%). The biotite/hornblende monzogranites (e.g., the Hepeng, the Luyang, the Zhuboyan, and the Qichuan) consist of quartz (22–27%), plagioclase (20–30%), K-feldspar (18–25%), biotite (3–8%), and amphibole (0–5%), and minor amounts of sphene, zircon, magnetite, and apatite. The biotite granites (e.g., the Baimajian) have quartz (25–28%), plagioclase (20–25%), K-feldspar (30–35%), biotite (3–5%), and accessory minerals including sphene, zircon, magnetite, monazite, and apatite. The granodiorites (e.g., the Sikongshan, the Zhuboyan, and the Qichuan) consist of quartz (15–20%), plagioclase (35–45%), K-feldspar (10–15%), biotite (5–8%), and amphibole (4–8%) and minor minerals including sphene, zircon, magnetite, and apatite. Most of the plutons have isotopic ages ranging from 112 to 129 Ma (Table 1). The Shanqi pluton lacks age data, but it is also regarded as a Cretaceous pluton because this pluton is characterized by the absence of foliation and tectonic deformation, similar to other Cretaceous granitoids.

#### 4. Analytical methods

After petrographic examination to insure freshness, 2–4 samples for representative pluton within different tectonic units have been picked out. Rock samples

were crushed in a specially designed steel jaw crusher and then powdered in an agate mill to a grain size <200 mesh. Analyses of major element compositions were made at the Analytical Institute of the Hubei Bureau of Geology and Mineral Resources. For the major elements,  $\text{SiO}_2$  and  $\text{H}_2\text{O}^+$  were determined by gravimetry;  $\text{TiO}_2$  and  $\text{P}_2\text{O}_5$  by spectrophotometry;  $\text{Al}_2\text{O}_3$ ,  $\text{Fe}_2\text{O}_3$ ,  $\text{FeO}$ , and  $\text{CO}_2$  by volumetry; and  $\text{MnO}$ ,  $\text{MgO}$ ,  $\text{CaO}$ ,  $\text{Na}_2\text{O}$ , and  $\text{K}_2\text{O}$  by atomic absorption spectrometry. The analytical uncertainty is usually <5% except for  $\text{H}_2\text{O}^+$  and  $\text{CO}_2$ . Trace elements, including rare earth elements (REE), were determined using the ICP-MS (POEMS 3) at China University of Geosciences. Two methods of sample digestion were used. In the alkali fusion, the glass was prepared by heating a mixture of sample and superpure  $\text{LiBO}_2$  in a proportion of 1:1 in Pt crucible in furnace for half an hour at a temperature of 1250 °C. In the acid digestion, a nominal 50-mg sample was dissolved in a mixture of HF and  $\text{HNO}_3$  in a Savillex screw-top Teflon breaker. The alkali fusion was used for analysis of Nb, Ta, Zr, and Hf, which are difficult to be dissolved because of host in zircon. The acid digestion was used for analysis of other trace elements. Rh and In were used as internal standard for correcting instrumental signal drift, which was usually <10% over a period of 6 h. Three international standard reference samples (G-2, JG-2, and AVG-1) were used to monitor daily accuracy and precision. As shown in Appendix A, analytical precision (relative standard deviation) was <5% for most elements except for Ni and Cu, which are 1–14%. Accuracy of the analysis, determined by comparisons to the recommended values of G-2, JG-2, and AVG-1 (Goveindaraju, 1994), is within 10% (Appendix A).

Sr–Nd–Pb isotopic data were obtained using a Finnegan MAT-261 multicollector mass spectrometer at China University of Geosciences. Sr and Nd isotopic fractionation was corrected to  $^{86}\text{Sr}/^{88}\text{Sr}=0.1194$  and  $^{146}\text{Nd}/^{144}\text{Nd}=0.7219$ , respectively. During the period of analysis, NBS987 standard and La Jolla standard yielded  $^{87}\text{Sr}/^{86}\text{Sr}=0.71025 \pm 4(2\sigma)$  and  $^{143}\text{Nd}/^{144}\text{Nd}=0.511853 \pm 9(2\sigma)$ , respectively. BCR-2 standard gave  $^{143}\text{Nd}/^{144}\text{Nd}=0.512638 \pm 5(2\sigma)$ . Total procedural Sr and Nd blanks are <1 ng and <50 pg, respectively. Detailed analytical procedure for the Sr and Nd isotopic measurements are given in Zhang et al. (1996) and Gao et al. (1999).

Table 2  
Major and trace element compositions of Cretaceous granitoids from Dabieshan

Sample <sup>a</sup>	DB163	DB165	DB168	DB171	DB177	DB211	DB216	DB218	DB220	DB232	DB233	DB240	DB242	DB248	DB251	DB254	DB260
	LY	LY	QC	QC	QC	SKS	SKS	BM	BM	ZB	ZB	ZB	ZB	SQ	SQ	HP	HP
SiO <sub>2</sub>	70.79	75.06	63.06	64.46	64.04	61.83	64.49	72.03	74.7	60.02	61.48	69.36	72.45	60.49	54.08	69.6	68.43
TiO <sub>2</sub>	0.38	0.19	0.63	0.67	0.59	0.76	0.67	0.30	0.18	0.93	0.84	0.45	0.30	0.95	1.06	0.49	0.56
Al <sub>2</sub> O <sub>3</sub>	14.42	13.09	14.64	14.81	14.82	17.39	16.49	14.27	13.45	16.93	16.16	15.18	13.72	15.64	16.39	14.25	14.7
Fe <sub>2</sub> O <sub>3</sub>	0.92	0.56	1.49	1.45	1.54	1.54	1.44	0.80	0.44	2.44	2.35	1.05	0.75	2.18	3.31	1.31	1.43
FeO	1.35	0.55	2.85	2.57	2.85	3.32	2.70	1.05	0.68	3.78	3.25	1.18	1.02	3.25	4.92	1.42	1.65
MnO	0.04	0.02	0.06	0.05	0.08	0.07	0.06	0.03	0.03	0.08	0.10	0.05	0.04	0.10	0.16	0.05	0.06
MgO	0.79	0.36	4.00	2.99	3.20	1.81	1.48	0.54	0.31	2.26	2.28	0.65	0.47	2.94	4.56	1.05	1.18
CaO	1.91	1.16	4.14	3.57	4.13	3.82	3.38	1.52	1.12	4.66	4.62	1.49	1.34	4.61	7.62	2.17	2.35
Na <sub>2</sub> O	3.70	3.50	4.24	4.21	3.83	4.87	4.64	3.53	3.63	4.27	4.07	4.38	3.92	3.99	3.46	4.01	3.94
K <sub>2</sub> O	4.71	4.76	3.30	3.70	3.46	3.08	3.30	5.10	4.86	3.08	3.30	5.33	5.13	3.90	2.02	4.57	4.61
P <sub>2</sub> O <sub>5</sub>	0.13	0.04	0.29	0.29	0.24	0.34	0.31	0.09	0.03	0.37	0.33	0.11	0.09	0.38	0.46	0.18	0.20
CO <sub>2</sub>	0.04	0.04	0.04	0.07	0.07	0.04	0.04	0.04	0.04	0.04	0.04	0.04	0.04	0.07	0.14	0.11	0.04
H <sub>2</sub> O	0.59	0.48	0.92	0.84	0.88	0.78	0.68	0.46	0.33	0.83	0.91	0.50	0.52	1.21	1.54	0.55	0.59
Total	99.77	99.81	99.66	99.68	99.73	99.65	99.68	99.76	99.8	99.69	99.73	99.77	99.79	99.71	99.72	99.76	99.74
K <sub>2</sub> O/Na <sub>2</sub> O	1.27	1.36	0.78	0.88	0.90	0.63	0.71	1.44	1.34	0.72	0.81	1.22	1.31	0.98	0.58	1.14	1.17
A/CNK	0.98	1.01	0.81	0.85	0.84	0.95	0.95	1.01	1.01	0.90	0.87	0.97	0.95	0.82	0.75	0.92	0.93
Sc	2.8	1.6	12.2	2.1	2.7	6.9	5.5	0.3	1.8	6.1	12.9	1.1	13.9	14.1	31.0	4.6	0.6
V	24	9.9	99	86	103	86	63	19	7.7	121	112	33	117	119	205	39	46
Cr	9.0	2.2	225.9	154.1	167.8	13.0	9.9	5.4	1.5	21.3	18.8	3.9	56.8	58.5	89.5	10.0	11.0
Co	4.1	1.7	24	16	22	14	9.9	3.1	1.3	21	19	5.9	23	24	35	6.8	8.3
Ni	4.8	2.0	99	58	62	10	7.6	4.2	2.4	13	14	5.9	38	39	26	8.7	9.1
Cu	18	3.6	27	14	24	25	18	7.9	14	26	26	14	36	37	33	9.9	11
Zn	33	33	67	46	56	72	65	39	25	91	72	73	68	70	86	50	78
Ga	17.1	17.3	20.8	18.7	20.8	24.4	20.4	19.7	19.4	24.6	21.2	22.6	22.4	23.2	21.4	20.7	20.2
Rb	145	180	88	62	73	59	65	149	162	81	76	193	265	117	47	207	180
Sr	384	182	1373	1030	786	1148	1007	368	239	900	836	264	236	775	898	474	556

Y	12.2	1.6	10.9	3.7	8.1	18.4	18.5	3.7	11.1	17.8	24.7	10.7	25.9	26.5	33.6	26.2	5.7
Zr	202	104	192	150	189	258	275	223	118	327	279	361	233	341	190	237	280
Nb	16.2	6.5	8.6	8.3	9.2	10.8	11.8	10.2	12.6	11.8	11.5	30.9	19.3	15.6	8.6	20.1	18.9
Cs	0.61	1.66	2.70	0.31	1.07	0.70	0.84	1.66	1.49	0.56	0.65	1.88	1.50	1.48	0.84	3.77	1.27
Ba	1338	782	1903	1471	1547	2330	1903	1906	1041	2109	1921	1113	1801	1854	1657	1269	1416
Hf	5.69	3.24	4.82	6.33	4.84	6.98	7.13	5.59	2.21	8.04	6.45	9.35	5.98	7.70	2.66	6.04	7.29
Ta	1.09	0.32	0.41	0.40	0.42	0.61	0.68	0.60	0.81	0.69	0.49	1.54	0.87	0.80	0.40	0.91	0.92
Pb	27.0	28.5	31.8	24.7	28.3	13.2	14.6	33.4	45.3	16.5	16.1	27.7	15.7	15.9	10.0	31.1	30.2
Th	16.0	14.1	7.08	0.97	1.98	6.98	7.36	3.87	30.5	4.54	6.82	5.40	15.5	15.4	3.14	45.6	4.95
U	2.14	1.64	0.76	2.08	0.57	1.17	4.42	3.04	4.07	0.89	2.88	2.86	3.71	0.67	5.87	8.25	0.54
La	65.8	42.7	450.0	63.8	45.3	58.9	70.8	92.7	45.4	76.8	56.5	93.4	86.5	80.0	57.9	80.0	91.0
Ce	117	78.6	95.8	109	82.9	122	134	149	84.1	150	120	185	159	157	131	155	172
Pr	10.7	7.02	10.1	10.3	8.29	11.7	13.4	12.6	7.49	15.0	12.1	17.0	13.0	15.0	14.6	14.0	15.7
Nd	36.5	24.2	38.7	35.0	30.2	44.2	49.6	45.7	25.8	56.4	47.5	62.3	42.8	55.7	62.4	49.7	55.2
Sm	5.27	3.41	6.45	5.19	4.97	7.12	8.61	6.08	3.99	9.42	8.44	10.89	6.18	9.35	11.57	8.01	8.75
Eu	1.18	0.81	1.84	1.57	1.55	2.11	2.33	1.32	0.88	2.63	2.21	1.53	1.01	2.19	2.67	1.48	1.71
Gd	3.56	1.95	4.34	3.60	3.66	5.05	6.20	3.85	2.72	6.93	6.22	8.55	4.32	6.80	9.03	6.07	6.65
Tb	0.48	0.24	0.59	0.49	0.52	0.70	0.87	0.59	0.38	0.98	0.88	1.30	0.63	0.96	1.31	0.87	0.96
Dy	2.85	1.50	3.25	2.71	3.02	3.98	4.86	3.33	2.34	5.58	5.03	7.85	3.70	5.56	7.35	5.32	5.80
Ho	0.57	0.32	0.61	0.51	0.60	0.77	0.93	0.70	0.48	1.08	0.98	1.61	0.74	1.10	1.40	1.10	1.20
Er	1.51	0.87	1.51	1.24	1.55	1.95	2.32	1.82	1.32	2.74	2.50	4.34	1.96	2.85	3.48	3.01	3.23
Tm	0.19	0.12	0.18	0.15	0.20	0.24	0.28	0.26	0.17	0.34	0.31	0.57	0.25	0.36	0.42	0.40	0.43
Yb	1.22	0.76	1.07	0.87	1.21	1.45	1.68	1.41	1.13	2.05	1.89	3.66	1.58	2.22	2.51	2.59	2.75
Lu	0.18	0.12	0.15	0.12	0.17	0.19	0.23	0.22	0.15	0.25	0.26	0.52	0.21	0.30	0.33	0.36	0.40
La <sub>N</sub> /Yb <sub>N</sub>	36	38	31	50	25	27	28	44	27	25	20	17	37	24	16	21	22
Eu/Eu *	0.79	0.88	1.00	1.06	1.06	1.03	0.93	0.78	0.77	0.95	0.89	0.47	0.57	0.80	0.77	0.63	0.66
Nb/Ta	14.9	20.3	21.0	20.8	21.9	17.7	17.4	17.0	15.6	17.1	23.5	20.1	22.2	19.5	21.5	22.1	20.5
Zr/Nb	12.5	16.0	22.3	18.1	20.5	23.9	23.3	21.9	9.4	27.7	24.3	11.7	12.1	21.9	22.1	11.8	14.8
Th/U	7.5	8.6	9.3	0.5	3.5	6.0	1.7	1.3	7.5	5.1	2.4	1.9	4.2	23.0	0.5	5.5	9.2
Rb/Nb	9.0	27.7	10.2	7.5	7.9	5.5	5.5	14.6	12.9	6.9	6.6	6.2	13.7	7.5	5.5	10.3	9.5

<sup>a</sup> Pluton abbreviations as in Fig. 1. Major and trace elements are reported in weight percent and parts per million, respectively.

Pb was separated by an anion exchange in HCl–Br columns. According to Pb content of each sample, measured by ICP-MS, 120–250 mg of each sample was dissolved in Teflon-DFA bombs with HF and HNO<sub>3</sub>. Usually, 120–150 mg was for samples with Pb contents of > 15 ppm and 170–250 mg for samples with Pb contents of < 15 ppm. Pb isotopic ratios were measured on the same Finnegan MAT-261 mass spectrometer. Silica gel–phosphoric acid loading technique was used following the method of Pinarelli et al. (1993). Stable beams were obtained at filament temperatures of  $1200 \pm 50$  °C. All the Pb isotopic data were empirically corrected for thermal fractionation by 0.10% ( $\pm 0.01$ ) per mass unit, a value derived from the isotopic values measured for common lead standard NBS 981, run under the same conditions as the samples. During the course of this study, 25 measurements of common lead standard NBS 981 gave average values of  $^{206}\text{Pb}/^{204}\text{Pb} = 16.942 \pm 4(2\sigma)$ ,  $^{207}\text{Pb}/^{204}\text{Pb} = 15.498 \pm 4$  and  $^{208}\text{Pb}/^{204}\text{Pb} = 36.728 \pm 9$ . Duplicate analyses indicate their reproducibility better than 0.1%. Total procedural Pb blanks were in the range of 2–4 ng. It has a negligible effect on reported Pb

isotopic ratios since several micrograms of Pb were extracted for most of samples with Pb contents of > 15 ppm. In this case, the uncertainties are < 0.1% at the 95% confidence level for  $^{206}\text{Pb}/^{204}\text{Pb}$ ,  $^{207}\text{Pb}/^{204}\text{Pb}$ , and  $^{208}\text{Pb}/^{204}\text{Pb}$ . For samples with Pb content of < 15 ppm, Pb blank influence on the Pb isotopic ratios is generally < 0.3%. Even with a 0.3% uncertainty, it appears that the distinction and similarity in Pb isotopic composition between our samples still hold.

## 5. Results

### 5.1. Major and trace elements

Major and trace element compositions of the Cretaceous granitoids are given in Table 2. Sample DB251 is a diorite with SiO<sub>2</sub> = 54%, MgO = 4.6%, and CaO = 7.6%. For the convenience of discussion, this sample is added up to the category of granitoid. The Cretaceous granitoids display a large SiO<sub>2</sub> range from 54% to 73%. As shown in Fig. 2, major element variations exhibit linear trends: TiO<sub>2</sub>,  $\Sigma\text{FeO}$ , CaO, and P<sub>2</sub>O<sub>5</sub> contents

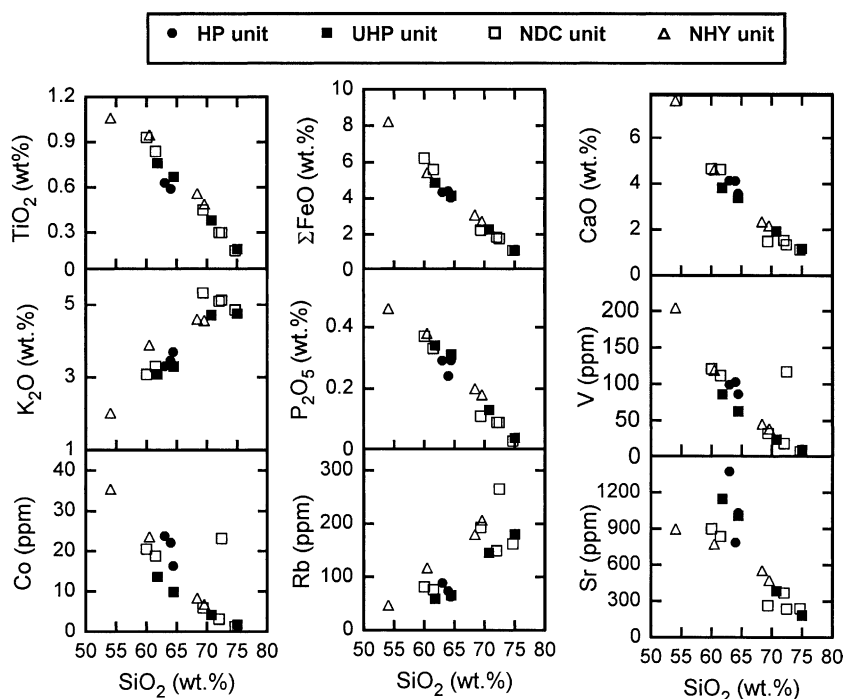


Fig. 2. Variations of major and trace element with SiO<sub>2</sub> for the Cretaceous granitoids from the eastern Dabieshan.



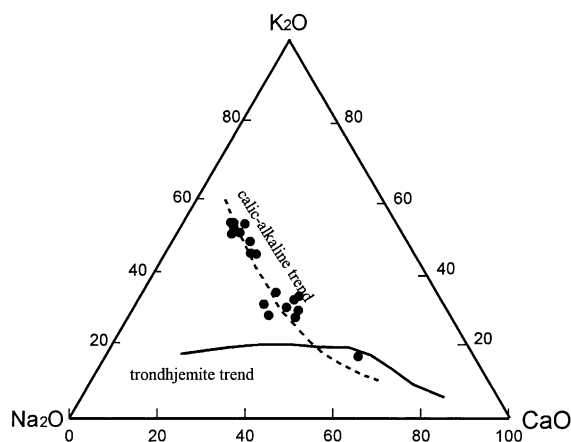


Fig. 3.  $K_2O$ – $Na_2O$ – $CaO$  diagram for the Cretaceous granitoids from the eastern Dabieshan. The calc-alkaline and trondhjemite trends are from Bark and Arth (1976).

decrease and  $K_2O$  contents increase with increasing  $SiO_2$  contents. This indicates that the Cretaceous granitoids might be derived from the similar magma source and the compositional variations result from partial melting and/or crystal fractionation, although they come from different tectonic units. This is strongly supported by Sr–Nd–Pb isotopic data (see below). The

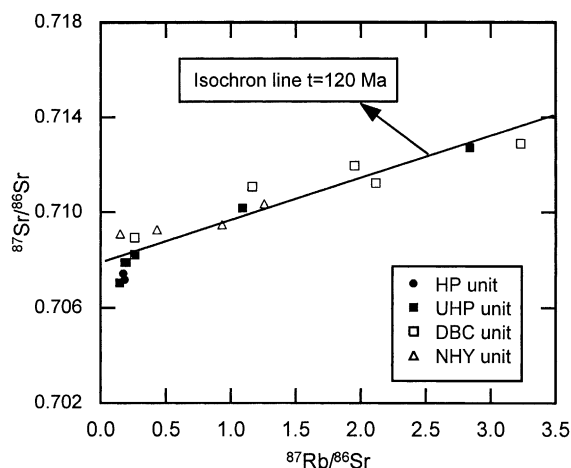


Fig. 5.  $^{87}Sr/^{86}Sr$  vs.  $^{87}Rb/^{86}Sr$  diagram for Cretaceous granitoids from the eastern Dabieshan.

$K_2O/Na_2O$  ratio ranges between 0.58 and 0.98 for samples with  $SiO_2 < 68\%$  and between 1.14 and 1.36 for the samples with  $SiO_2 > 68\%$ . Most samples have A/CNK [ $Al_2O_3/(CaO + Na_2O + K_2O)$  molecular ratio] values of 0.75–0.98. A few samples (DB165, DB218, and DB220) have A/CNK ratio of 1.01. Thus, the Cretaceous granitoids are predominantly metaluminous

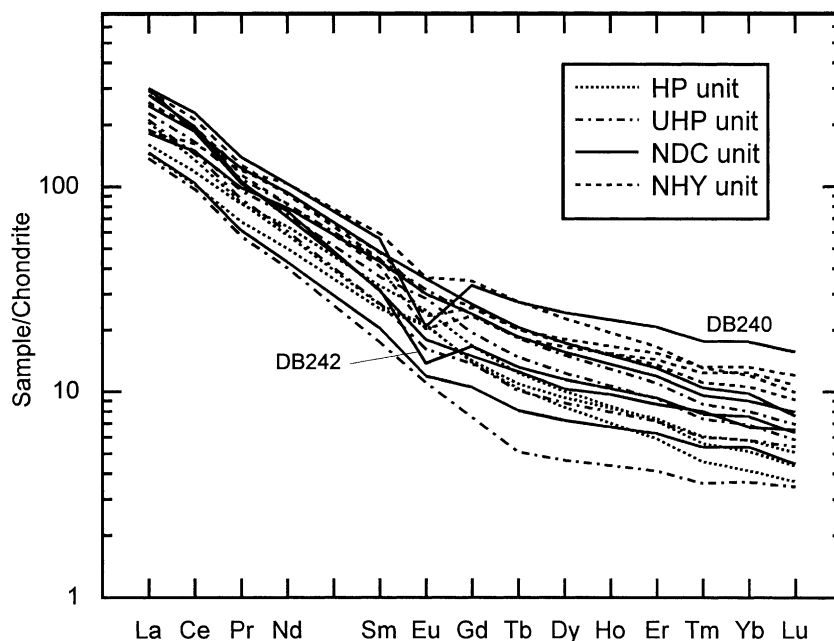


Fig. 4. Chondrite-normalized REE patterns for Cretaceous granitoids from the eastern Dabieshan.

and belong to I-type granitoids (White and Chappell, 1977). They exhibit a calc-alkaline trend in the  $K_2O$ – $Na_2O$ – $CaO$  ternary diagram (Fig. 3).

Corresponding to the major element compositions, the trace element compositions also show large variations, some of which (e.g., Rb, V, Co, and Sr) correlate well with  $SiO_2$  (Fig. 2). Samples with  $SiO_2 < 68\%$  mostly have 47–117 ppm Rb and 775–1371 ppm Sr, while samples with  $SiO_2 > 68\%$  have 145–265 ppm Rb and 182–556 ppm Sr. Other incompatible trace elements display more scattered variations (e.g., Nb = 1.1–30.9 ppm, Ta = 0.1–1.5 ppm, Zr = 42–327 ppm, Hf = 1.4–9.4 ppm, Th = 1.7–45.6 ppm, and U = 0.8–8.3 ppm) with  $SiO_2$ . However, the Cretaceous granitoids of the four tectonic units show overlapped Nb/Ta, Zr/Nb, Th/U, and Rb/Nb ratios (Table 2).

REE distributions for the Cretaceous granitoids are shown in Fig. 4. The samples from different tectonic units exhibit similar and strongly fractionated REE patterns with  $La_N/Yb_N = 13$ –44, irrespective of their rock type, again suggesting that their source and formation and evolution processes are similar. The granitoids from the UHP and HP units show no obvious Eu anomalies with  $(Eu^*/Eu) = 0.79$ –1.06. Samples DB218, DB220, and DB233 from the NDC unit have  $Eu^*/Eu$  values ranging from 0.77 to 0.95, which are similar to those of the UHP and HP units. Samples DB240 and DB242 (Zhubuyan pluton) from the NDC unit have medium negative Eu anomalies with  $Eu^*/Eu$  values of 0.47 and 0.57, respectively. This indicates that some samples in the NDC unit experienced the process of magma fractionation crystallization. Sam-

Table 3

Rb–Sr and Sm–Nd isotopic compositions of Dabieshan Cretaceous granitoids from different tectonic units

Sample	Rb (ppm)	Sr (ppm)	$^{87}Rb/^{86}Sr$	$^{87}Sr/^{86}Sr$	$\pm 2\sigma$	$(^{87}Sr/^{86}Sr)_t$	Sm (ppm)	Nd (ppm)	$^{147}Sm/^{144}Nd$	$^{143}Nd/^{144}Nd$	$\pm 2\sigma$	$\epsilon_{Nd}(0)$	$\epsilon_{Nd}(t)$	$T_{DM}$ (Ga)
<i>HP unit</i>														
DB168	85.42	1365.5	0.1857	0.70717	7	0.70685	5.51	35.12	0.0948	0.511624	9	–19.8	–18.2	2.0
DB171	64.21	1035.7	0.1740	0.70743	6	0.70713	4.93	34.06	0.0875	0.511814	14	–16.1	–14.4	1.6
DB177	70.96	790.1	0.2675	0.70819	9	0.70773	4.90	30.36	0.0976	0.511700	16	–18.3	–16.8	1.9
<i>UHP unit</i>														
DB163	142.43	380.4	1.0910	0.71017	8	0.70831	6.67	45.65	0.0883	0.511240	8	–27.3	–25.6	2.3
DB163 <sup>a</sup>	141.20	381.3	1.0901	0.71013	7	0.70828	6.65	45.78	0.0879	0.511248	7	–27.1	–25.5	2.3
DB165	178.58	185.5	2.8393	0.71272	7	0.70788	3.57	26.29	0.0821	0.511540	9	–21.4	–19.7	1.9
DB211	62.58	1155.3	0.1471	0.70704	9	0.70679	8.37	54.83	0.0923	0.511663	9	–19.0	–17.4	1.9
DB216	68.19	1021.9	0.1865	0.7079	8	0.70758	8.77	55.79	0.0950	0.511548	9	–21.3	–19.7	2.1
<i>DBC unit</i>														
DB218	150.57	362.8	1.1651	0.71107	7	0.70908	6.75	50.32	0.0811	0.511289	9	–26.3	–24.6	2.1
DB220	166.56	245.6	1.9533	0.71196	5	0.70863	4.90	31.01	0.0955	0.511325	9	–25.6	–24.1	2.3
DB232	85.26	906.0	0.2604	0.70893	6	0.70849	10.10	61.87	0.0987	0.511305	11	–26.0	–24.5	2.4
DB233	81.12	845.9	0.2622	0.70822	6	0.70777	9.29	54.71	0.1026	0.511489	7	–22.4	–21.0	2.3
DB233 <sup>a</sup>	80.18	844.8	0.2619	0.70825	6	0.70780	9.04	52.53	0.1040	0.511482	8	–22.6	–21.1	2.3
DB240	190.63	270.9	2.1162	0.71122	8	0.70761	11.60	66.86	0.1048	0.511780	9	–16.7	–15.3	1.9
DB242	260.71	231.2	3.2321	0.71289	4	0.70738	6.71	44.79	0.0905	0.511629	9	–19.7	–18.1	1.9
<i>NHY unit</i>														
DB248	121.51	788.4	0.4332	0.70927	8	0.70853	9.58	59.10	0.0980	0.511874	10	–14.9	–13.4	1.7
DB251	51.74	907.5	0.1502	0.7091	5	0.70884	10.97	61.62	0.1076	0.511755	7	–17.2	–15.9	2.0
DB254	203.23	478.7	1.2589	0.71036	7	0.70821	8.18	52.93	0.0934	0.511665	10	–19.0	–17.4	1.9
DB260	175.08	542.0	0.9339	0.70948	6	0.70789	8.65	55.26	0.0946	0.511707	9	–18.2	–16.6	1.8

<sup>a</sup> Duplicate analyses.  $(^{87}Sr/^{86}Sr)_t$  and  $\epsilon_{Nd}(t)$  calculations use the mean emplacement age of 120 Ma for the Cretaceous granitoids with present-day  $(^{147}Sm/^{144}Nd)_{CHUR} = 0.1967$  and  $(^{143}Nd/^{144}Nd)_{CHUR} = 0.512638$  and  $T_{DM}$  calculations use present-day  $(^{147}Sm/^{144}Nd)_{DM} = 0.2137$  and  $(^{143}Nd/^{144}Nd)_{DM} = 0.51315$ .

ples from the NHY unit display  $\text{Eu}^*/\text{Eu}$  values of 0.63–0.83.

### 5.2. Sr and Nd isotopes

In  $^{87}\text{Rb}/^{86}\text{Sr}$  vs.  $^{87}\text{Sr}/^{86}\text{Sr}$  diagram (Fig. 5), the granitoid samples from different units display a linear distribution. They are close to an isochrone line with  $t = 120$  Ma. This is in good agreement with their magma emplacement ages ranging from 112 to 129 Ma (Table 1). For the purpose of comparison, all samples are calculated for initial  $(^{87}\text{Sr}/^{86}\text{Sr})_i$  ratios using a mean magma emplacement age of 120 Ma (Table 3). Samples from the HP and UHP units have the initial  $(^{87}\text{Sr}/^{86}\text{Sr})_i$  ratios of 0.7069–0.7077 and 0.7068–0.7083, respectively. Samples from the NDC and the NHY units have the initial  $(^{87}\text{Sr}/^{86}\text{Sr})_i$  ratios of 0.7074–0.7091 and 0.7079–0.7089, respectively. This result indicates that the granitoids from four tectonic units have similar

initial  $(^{87}\text{Sr}/^{86}\text{Sr})_i$  ratios, showing that their magma sources are alike and resemble I-type granitoids (White and Chappell, 1977).

The Cretaceous granitoids show a slight heterogeneity in Nd isotopic composition (Table 3). The measured  $^{143}\text{Nd}/^{144}\text{Nd}$  ratios range from 0.511240 to 0.511874 and  $^{147}\text{Sm}/^{144}\text{Nd}$  ratios from 0.0821 to 0.1076. They display a large variation range in  $\varepsilon_{\text{Nd}}(t)$  from  $-13$  to  $-26$ , which agrees with the range ( $\varepsilon_{\text{Nd}}(t) = -14$  to  $-22$ ) for the Dabie Cretaceous granitoids obtained by Ma et al. (1998). The results indicate that they are mostly products of partial melting of continental materials. It should be noted that the Cretaceous granitoids, irrespective of tectonic unit and rock type, have a similar  $\varepsilon_{\text{Nd}}(t)$  range. This strongly suggests a similar source composition for the Cretaceous granitoids from the four tectonic units.

Nd model ages ( $T_{\text{DM}}$ ) represent the time when source of a rock is extracted from a model-depleted

Table 4  
Whole-rock Pb isotopic ratios for Dabieshan Cretaceous granitoids from different units

Sample	$^{206}\text{Pb}/^{204}\text{Pb}$	$^{207}\text{Pb}/^{204}\text{Pb}$	$^{208}\text{Pb}/^{204}\text{Pb}$	Pb (ppm)	Th (ppm)	U (ppm)	$(^{206}\text{Pb}/^{204}\text{Pb})_i$	$(^{207}\text{Pb}/^{204}\text{Pb})_i$	$(^{208}\text{Pb}/^{204}\text{Pb})_i$
<i>HP unit</i>									
DB168	16.521	15.269	36.937	31.77	7.08	0.76	16.494	15.268	36.854
DB168 <sup>a</sup>	16.515	15.263	36.932						
DB171	16.718	15.345	37.190	24.65	0.97	2.08	16.622	15.340	37.175
DB177	16.457	15.300	36.912	28.25	1.98	0.57	16.434	15.299	36.886
<i>UHP unit</i>									
DB163	15.619	15.209	36.592	27.03	16.04	2.14	15.531	15.205	36.376
DB165	16.506	15.242	37.305	28.47	14.14	1.64	16.440	15.239	37.120
DB211	16.575	15.250	37.181	13.20	6.89	1.17	16.575	15.250	37.181
DB216	16.426	15.246	37.292	14.56	7.36	4.42	16.081	15.229	37.104
<i>NDC unit</i>									
DB218	16.237	15.265	37.296	33.44	3.87	3.04	16.134	15.260	37.253
DB220	16.320	15.263	37.248	45.29	30.54	4.07	16.218	15.258	36.997
DB232	16.201	15.258	37.206	16.54	4.54	0.89	16.140	15.255	37.104
DB232 <sup>a</sup>	16.235	15.260	37.216						
DB233	16.114	15.240	37.034	16.08	6.82	2.88	15.912	15.230	36.878
<i>NHY unit</i>									
DB248	16.975	15.438	37.805	15.86	15.36	0.67	16.926	15.436	37.438
DB251	17.063	15.430	37.627	9.95	3.14	5.87	16.381	15.397	37.507
DB251 <sup>a</sup>	16.045	15.428	37.623						
DB254	16.781	15.394	37.521	31.09	45.57	8.25	16.476	15.379	36.970
DB260	16.707	15.375	37.443	30.19	4.95	0.54	16.686	15.374	37.382

<sup>a</sup> Duplicate analyses. Initial Pb isotopic ratios [ $(^{206}\text{Pb}/^{204}\text{Pb})_i$ ,  $(^{207}\text{Pb}/^{204}\text{Pb})_i$ , and  $(^{208}\text{Pb}/^{204}\text{Pb})_i$ ] are calculated using the measured whole-rock Pb isotopic compositions, whole-rock U, Th, and Pb contents, and the age of 120 Ma.

mantle reservoir, assuming that there were no fractionation of Sm from Nd subsequent to separation from the mantle (Arndt and Goldstein, 1987; Milisenda et al., 1994). Although this assumption is difficult to

demonstrate for granitic rocks derived from crustal sources, the Nd model age of granitoids is considered to constrain the residence age of their source in the continental crust (Arndt and Goldstein, 1987). The

Table 5  
Whole-rock Pb isotopic data from the Northern Dabie complex and UHP units

Sample	$^{206}\text{Pb}/^{204}\text{Pb}$	$^{207}\text{Pb}/^{204}\text{Pb}$	$^{208}\text{Pb}/^{204}\text{Pb}$	Pb (ppm)	Th (ppm)	U (ppm)	$(^{206}\text{Pb}/^{204}\text{Pb})_t$	$(^{207}\text{Pb}/^{204}\text{Pb})_t$	$(^{208}\text{Pb}/^{204}\text{Pb})_t$
<b>NDC unit</b>									
<i>Orthogneiss</i>									
DB-135	16.929	15.340	37.731	26.38	1.16	1.35	16.870	15.337	37.714
DB-142	16.534	15.276	37.455	20.15	8.70	0.60	16.500	15.274	37.294
DB-142 <sup>a</sup>	16.542	15.279	37.464						
DB-224	16.047	15.247	36.999	27.62	1.12	1.41	15.989	15.244	36.984
DB-229	16.538	15.288	37.310	25.14	16.52	2.84	16.409	15.282	37.065
<i>Amphibolite</i>									
DB-130	17.308	15.414	37.846	9.97	0.72	0.63	17.235	15.410	37.819
DB-133	16.622	15.460	37.968	20.06	6.48	0.90	16.570	15.457	37.846
DB-176	16.034	15.221	36.926	18.14	2.03	0.32	16.014	15.220	36.885
DB-179	15.845	15.158	36.778	15.76	3.18	0.46	15.812	15.156	36.704
DB-179 <sup>a</sup>	15.857	15.152	36.789						
DB-337	17.081	15.386	37.896	33.51	2.53	0.83	17.052	15.385	37.867
DB-357	16.802	15.325	37.858	12.47	3.57	0.71	16.736	15.322	37.750
DB-357 <sup>a</sup>	16.786	15.320	37.842						
DB-359	16.629	15.328	37.741	13.13	0.95	0.38	16.596	15.326	37.714
<b>UHP unit</b>									
<i>Gneiss</i>									
DB-21	17.452	15.321	37.552	11.72	3.89	0.62	17.391	15.318	37.426
DB-290	17.428	15.547	38.048	27.23	2.79	1.29	17.372	15.544	38.009
DB-303	17.398	15.398	37.898	7.54	3.32	1.54	17.160	15.386	37.730
DB-305	19.872	15.741	42.833	2.07	10.30	1.09	19.192	15.708	40.727
DB-305 <sup>a</sup>	19.848	15.770	42.633						
DB-309	17.900	15.445	37.691	3.31	1.27	2.02	17.184	15.410	37.544
SM-1	17.955	15.506	38.296	8.21	2.98	0.48	17.886	15.503	38.156
D95-39	18.883	15.531	38.208	8.44	3.13	0.54	18.806	15.527	38.063
DB-306	17.426	15.428	37.965	45.33	7.58	1.63	17.384	15.426	37.901
DB-24	17.507	15.490	37.826	25.35	5.10	0.85	17.468	15.488	37.749
R-69	17.845	15.539	38.187	60.81	5.48	0.87	17.828	15.538	38.152
R316-2	17.978	15.542	38.194	83.42	2.51	0.41	17.972	15.542	38.182
BXL99	17.660	15.422	38.088	24.65	2.85	0.99	17.613	15.420	38.044
R-24	17.768	15.506	38.077	50.12	8.40	0.96	17.745	15.505	38.013
R-70	17.979	15.540	38.234	38.24	7.40	1.60	17.930	15.538	38.159
<i>Eclogite</i>									
D95-38	17.587	15.450	38.010	13.9	5.95	1.53	17.458	15.444	37.846
SH02	17.308	15.393	37.808	7.99	0.82	0.72	17.203	15.388	37.769
SH02 <sup>a</sup>	17.296	15.398	37.838						
XD98-1	17.237	15.376	37.590	32.2	1.12	0.34	17.225	15.375	37.577
D97-17	17.761	15.452	38.020	5.99	2.93	0.84	17.596	15.444	37.832
D95-24	17.830	15.532	38.015	7.73	0.72	0.12	17.812	15.531	37.979

<sup>a</sup> Duplicate analyses.  $(^{206}\text{Pb}/^{204}\text{Pb})_t$ ,  $(^{207}\text{Pb}/^{204}\text{Pb})_t$ , and  $(^{208}\text{Pb}/^{204}\text{Pb})_t$  are Pb isotopic ratios at  $t=120$  Ma. The calculations use the measured whole-rock U, Th, and Pb contents and whole-rock Pb isotopic ratios.

Cretaceous granitoids have  $T_{DM}$  of 1.6–2.4 Ga, which is much older than their emplacement ages. This suggests that their sources are Precambrian in age.

### 5.3. Pb isotope

The Cretaceous granitoids are characterized by less radiogenic Pb isotopic compositions (Table 4). Their present-day whole-rock Pb isotopic compositions are characterized by  $^{206}\text{Pb}/^{204}\text{Pb} = 15.6–17.1$ ,  $^{207}\text{Pb}/^{204}\text{Pb} = 15.2–15.5$ , and  $^{208}\text{Pb}/^{204}\text{Pb} = 36.6–37.8$ , which resemble the lower crustal Pb isotopic composition (Zartman and Doe, 1981). The present-day Pb isotopic ratios are calculated to the composition at the time of emplacement using whole-rock U, Th, and Pb contents and the age of 120 Ma. The derived initial Pb isotopic compositions are  $(^{206}\text{Pb}/^{204}\text{Pb})_i = 15.5–16.9$ ,  $(^{207}\text{Pb}/^{204}\text{Pb})_i = 15.2–15.5$ , and  $(^{208}\text{Pb}/^{204}\text{Pb})_i = 36.3–37.5$ , which are not significantly different from the present ratio because of their young age and

relatively low Th and U concentrations (Table 2). The calculated initial Pb isotopic compositions using whole-rock samples are similar to the feldspar Pb isotopic compositions of the Dabie Cretaceous granitoids, the latter having  $(^{206}\text{Pb}/^{204}\text{Pb})_i = 15.4–17.3$ ,  $(^{207}\text{Pb}/^{204}\text{Pb})_i = 15.1–15.5$ , and  $(^{208}\text{Pb}/^{204}\text{Pb})_i = 36.4–38.1$  (Zhang, 1995).

The NDC and UHP metamorphic rocks were also measured for whole-rock Pb isotopic analyses (Table 5). In the NDC, orthogneiss and amphibolite have similar Pb isotopic compositions with  $^{206}\text{Pb}/^{204}\text{Pb} = 16.0–17.3$ ,  $^{207}\text{Pb}/^{204}\text{Pb} = 15.2–15.5$ , and  $^{208}\text{Pb}/^{204}\text{Pb} = 36.8–37.9$ , which are similar to those of the Cretaceous granitoids. In the UHP, the gneiss and eclogite have more variable Pb isotopic compositions with  $^{206}\text{Pb}/^{204}\text{Pb} = 17.2–19.9$ ,  $^{207}\text{Pb}/^{204}\text{Pb} = 15.3–15.7$ , and  $^{208}\text{Pb}/^{204}\text{Pb} = 37.5–42.8$ . It is more distinctive that the samples from the NDC have lesser radiogenic Pb isotopic compositions than those from the UHP.

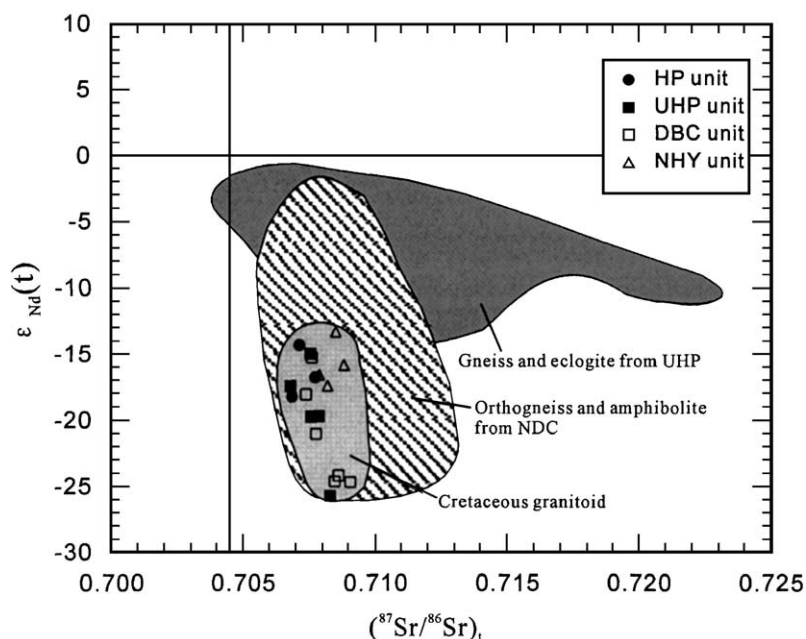


Fig. 6.  $\epsilon_{\text{Nd}}(t)$  vs.  $(^{87}\text{Sr}/^{86}\text{Sr})_t$  diagram for the Cretaceous granitoids. Each sample is calculated at  $t = 120$  Ma, a mean magma emplacement age for the Cretaceous granitoids. Also shown for comparison is the fields for the Northern Dabie complex and the UHP metamorphic rocks at  $t = 120$  Ma. The fields are delineated from coupled Sr and Nd data by Chen and Jahn (1998), Jahn (1998), Ma et al. (2000), and Zheng et al. (2000). The Cretaceous granitoids, irrespective of tectonic unit, show identical Sr–Nd isotopic compositions, which agree with the NDC and differ distinctly from the UHP metamorphic rocks.

## 6. Discussions

### 6.1. Magma source

The resemblance in major and trace composition, REE distribution, and Sr–Nd–Pb isotopic compositions of the Cretaceous granitoids suggest a similar source. It has been proposed from geochemical and isotopic evidence that the Cretaceous granitoids are product of partial melting of the Dabie complex (Li and Wang, 1991; Xu et al., 1994; Ma et al., 1998). Traditionally, the Dabie complex includes the Northern Dabie complex with no indication of UHP or HP metamorphism and the UHP metamorphic unit. For studies of tectonic framework and crustal structure, it is critical to distinguish whether the source of the Cretaceous granitoids is the Northern Dabie complex or the UHP unit. Fortunately, present data indicate that these two units can be clearly distinguished in Sr–Nd–Pb isotopic compositions.

According to Sr–Nd isotopic data (Chen and Jahn, 1998; Jahn, 1998; Ma et al., 2000; Zheng et al., 2000),  $\epsilon_{\text{Nd}}(t)$  and  $(^{87}\text{Sr}/^{86}\text{Sr})_t$  values for the Northern Dabie complex and the UHP metamorphic rocks are calcu-

lated at  $t = 120$  Ma, a mean magma emplacement for the Cretaceous granitoids. As shown in Fig. 6, although the Northern Dabie complex, which is dominated by orthogneiss and amphibolite, overlaps the UHP metamorphic rocks (eclogite and gneiss) in some extent, the Northern Dabie complex is characterized by more negative  $\epsilon_{\text{Nd}}(t)$  values and more narrow  $(^{87}\text{Sr}/^{86}\text{Sr})_t$  variation. In contrast to the Northern Dabie complex and the UHP metamorphic rocks, the samples from the Cretaceous granitoids totally overlap the Northern Dabie complex and are distinctly different from the UHP metamorphic rocks. The Sr–Nd isotopic composition of the Cretaceous granitoids from four tectonic units can be interpreted as resulting from the anatexis of the Northern Dabie complex in which the proportion of mantle-derived component is very small or even absent. This is true also for the Pb isotopic compositions. As illustrated in Fig. 7, the Cretaceous granitoids and the NDC show indistinguishable Pb isotopic compositions at the time of emplacement (120 Ma), which is, however, distinctly less radiogenic than the UHP metamorphic rocks. Pb isotopic tracing also clearly indicates that the magma source for the Cretaceous granitoids is the Northern Dabie complex.

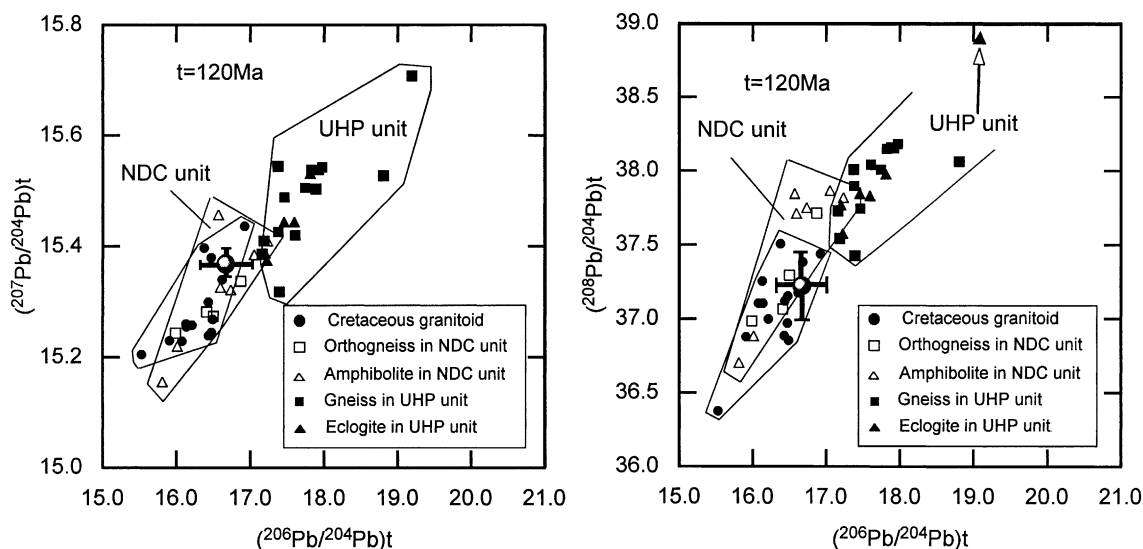


Fig. 7.  $(^{206}\text{Pb}/^{204}\text{Pb})_t$  vs.  $(^{207}\text{Pb}/^{204}\text{Pb})_t$  and  $(^{208}\text{Pb}/^{204}\text{Pb})_t$  diagrams for the Cretaceous granitoids, the Dabie core complex, and the UHP metamorphic complex. Pb isotopic ratios are calculated at the time of emplacement of the Cretaceous granitoids ( $t = 120$  Ma). The large ball with error bars indicates the average values of feldspar Pb isotopic compositions of the Dabie Cretaceous granitoids and one sigma deviation compiled by Zhang (1995). Like the Sr–Nd isotopic composition (Fig. 6), Pb isotopes of the Cretaceous granitoids, irrespective of tectonic unit, show similar composition, which again overlap with that of the NDC unit but differ distinctly from that of the UHP unit.

## 6.2. Crustal structure

As stated above, the Cretaceous granitoids were derived from crustal anatexis. They provide a probe for source composition of the deep crust, which, in turn, constrains the deep crustal structure. Although the Cretaceous granitoids are distributed in all the four tectonic units in the eastern Dabieshan, they share a similar source from the NDC. This fact implies that the exposed NDC unit must extend southward beneath the UHP/HP metamorphic unit and northward beneath the NHY unit. This means that the middle-lower crust of the four tectonic units, where the Cretaceous granitoids originated, is dominated by rocks having geochemical and Sr–Nd–Pb isotopic compositions similar to the NDC. Thus, the UHP/HP unit is confined to shallower crustal level and shows a thin skin structure over the NDC.

Above crustal structure is also confirmed by the Pb isotopic composition for the NDC and the UHP metamorphic rocks. According to Pb isotopic compositional variation in crustal vertical section (Zartman and Doe, 1981; Taylor and McLennan, 1985), lower crust has radiogenic Pb isotopic composition less than the upper crust because the lower crust is depleted in U and Th relative to the upper crust. The fact that the NDC has radiogenic Pb isotopic composition less than the UHP rocks indicates that the NDC underlies the UHP unit in the crustal structure. In the Triassic, the UHP unit was subducted northward into mantle depths and experienced UHP metamorphism, whereas the NDC was not subducted to mantle depth. During the exhumation of the UHP slab from mantle to crust,

the UHP slab was thrust upward and returned to the top of the NDC. Thus, the relative location between the NDC and the UHP slab was not changed before the UHP metamorphism and after the UHP exhumation. The UHP metamorphism might lead to the depletion of U and Th. However, the time effect on Pb isotopic composition is not obvious because of short time evolution from the Triassic to present. If rocks from the UHP unit did not undergo UHP metamorphism, the rocks would have more radiogenic Pb isotopic composition than observed present Pb isotopic composition.

In the overall context, the Northern Dabie complex is a core of dome within the Dabie orogenic belt, which was formed in lithospheric tectonic extension and post the UHP/HP metamorphism. The dome structure suggested by the present study (Fig. 8) is consistent with the tectonic model for post UHP/HP metamorphism from surface geology (Faure et al., 1999; Suo et al., 2000). It also agrees with the results of recent seismic refraction traversing the eastern Dabieshan and measurements of petrophysical properties of eclogites and associated rocks that the UHP/HP rock is not volumetrically significant in the middle or lower crust (Kern et al., 1999; Wang et al., 2000). Our geochemical study provides an independent evidence for the crustal structure of the Dabie UHP metamorphic terrain.

## 6.3. Tectonic implications

Many workers (Cong et al., 1996; Zhai and Cong, 1996; Wang and Cong, 1996) emphasized that the

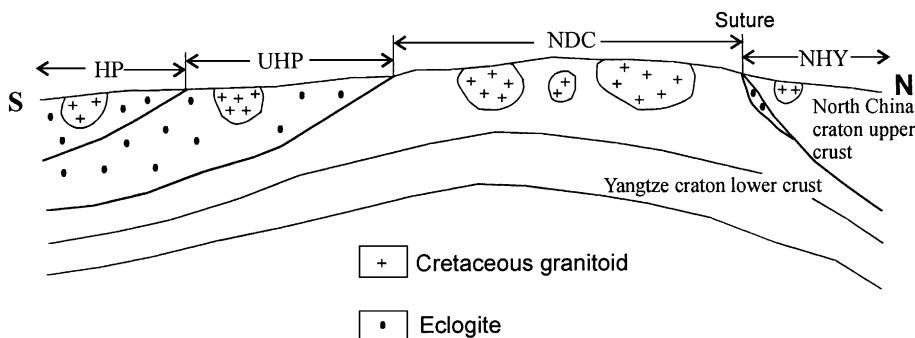


Fig. 8. A cartoon showing tectonic framework and crustal structure at the time of magma emplacement of the Cretaceous granitoids in the eastern Dabieshan. Symbols are the same as in Fig. 1.

Wuhe–Shuiko Fault separating the Northern Dabie complex and the UHP metamorphic unit is the suture between the North China and Yangtze cratons. They considered that the Northern Dabie complex is the root of an island-arc complex developed along the southern margin of the North China craton and the UHP metamorphic unit (the Southern Dabie complex) was subducted beneath the Northern Dabie complex. However, our results suggest that the UHP metamorphic unit is only a thin-skinned slab over the Northern Dabie complex and that both the northern and southern sides of the Wuhe–Shuiko Fault are underlain by the same basement of the Northern Dabie complex (Fig. 8). In this context, the Wuhe–Shuiko Fault is unlikely to be the suture between the North China craton and the Yangtze craton. The suture must be located further to the north of the Northern Dabie complex because the Northern Dabie complex has an affinity to the Yangtze craton (Hacker et al., 1998, 2000; Ratschbacher et al., 2000). This is consistent with the Nd isotopic model ages ( $T_{DM}$ ) of 1.6–2.4 Ga for the Cretaceous granitoids. As the North China craton is an Archean craton and the Yangtze craton is mainly a Proterozoic craton, although Archean rocks have been found recently (Qiu et al., 2000), the model ages also imply that the sources of the Cretaceous granitoids are from the Yangtze craton. The major evidence used to support the Wuhe–Shuiko Fault as the suture is the apparent lack of eclogites in the Northern Dabie complex. However, recent findings of eclogites in the Northern Dabie complex (Wei et al., 1997; Xu et al., 1999; Tsai and Liou, 2000) invalidated the assumption. In fact, the Wuhe–Shuiko Fault is a lower detachment zone surrounding the Northern Dabie complex related to the extension tectonics during the UHP rock exhumation (Suo et al., 2000), which is similar to the extensional tectonic framework of the UHP metamorphic terrain in southern Norway (Anderson, 1998). The Foziling Group in the north of the Xiaotian–Mozitang Fault experienced only greenschist-facies metamorphism. In contrast, the eclogites in the south experienced UHP or HP metamorphism. Based on the large contrast in metamorphic grade in both sides of the Xiaotian–Mozitang Fault, we propose that this fault marks the suture between the North China and Yangtze cratons. Thus, the shallow crust of the North Huaiyang block consists of the North China Paleozoic sedimentary rocks,

while the deep crust is the subducted Yangtze craton dominated by the Northern Dabie complex (Fig. 8). Recent geological and geochronological studies (Hacker et al., 1998, 2000; Suo et al., 1999; Ratschbacher et al., 2000) lead to a similar conclusion. This suture was significantly modified during the exhumation of the UHP metamorphic rocks. The above scenario is similar to intracontinent subduction in the Qinling orogenic belt to the west (Zhang et al., 1997).

## 7. Conclusion

Geochemical and Sr–Nd–Pb isotopic compositions of the Cretaceous granitoids from the four tectonic units in the Dabieshan indicate a similar crustal source for their magma genesis. The source has Sr, Nd, and Pb isotopic compositions identical to the Northern Dabie complex, and is distinct from the UHP unit. The results strongly suggest that the exposed Northern Dabie complex extends in the deep crust southward beneath the UHP/HP metamorphic unit and northward beneath the North Huaiyang unit. The Northern Dabie complex is a core of the dome within the Dabie orogenic belt. The UHP/HP metamorphic unit is only a thin-skinned slab confined in the shallower crustal levels over the Northern Dabie complex unit. The similar source for the Cretaceous granitoids also points out that the Wuhe–Shuiko Fault is unlikely to be the suture between the North China and the Yangtze cratons, which is, however, suggested to be marked by the Xiaotian–Mozitang Fault.

## Acknowledgements

This study is financially supported by the Chinese Ministry of Science and Technology (grants G1999075506 and G1999043202) and the National Nature Science Foundation of China (grants 49794043 and 40073005) and the Open Laboratory of Constitution, Interaction, and Dynamics of the Crust–Mantle System, the Ministry of Land and Mineral Resource of China. We thank Jahn Bor-Ming and Bradley Hacker for improving the manuscript. Constructive and thorough reviews by V. Chavagnac, M. Sun and R.L. Rudnick are greatly appreciated.



**Appendix A**

## Analyses of international standard reference rocks by ICP-MS

Element	Isotope	G-2 ( <i>n</i> = 3)				JG-2 ( <i>n</i> = 3)				AGV-1 ( <i>n</i> = 3)			
		Rec	Obt	Std	RSD (%)	Rec	Obt	Std	RSD (%)	Rec	Obt	Std	RSD (%)
Sc	45	3.5	3.5	0.11	3.11	2.47	2.8	0.02	0.72	12.2	12.5	0.83	6.65
V	51	36	35	0.46	1.33	3	2.8	0.02	0.73	121	120	5.55	4.64
Cr	52	8.7	7.4	0.12	1.62	7.6	8.9	0.06	0.68	10.1	9.8	0.06	0.61
Co	59	4.6	4.7	0.08	1.71	4.3	4.36	0.16	3.67	15.3	16	0.23	1.46
Ni	60	5	5.3	0.61	11.51	2.1	2.6	0.03	1.17	16	16	0.80	4.88
Cu	65	11	12.1	0.15	1.24	0.4	0.6	0.08	13.56	60	59	2.29	3.87
Zn	66	86	86	2.19	2.54	12.7	15	0.2	1.34	88	90	0.41	0.46
Ga	71	23	22	0.65	2.90	19	18.8	0.34	1.81	20	20.4	0.10	0.49
Rb	85	170	158	0.93	0.59	297	292	4.03	1.38	67.3	71	3.48	4.91
Sr	88	478	475	8.16	1.72	16	16.5	0.09	0.55	662	643	6.17	0.96
Y	89	11	9.83	0.14	1.42	88.2	92	1.79	1.94	20	19.7	0.79	4.01
Zr	91	309	307	8.43	2.75	101	110	0.37	0.34	227	224	4.22	1.89
Nb	93	12	12.8	0.52	4.07	15	14.1	0.06	0.42	15	14.5	0.23	1.59
Cs	133	1.34	1.35	0.01	0.74	7.5	8.0	0.09	1.13	1.28	1.21	0.03	2.48
Ba	135	1882	1824	15.22	0.83	67	68.4	0.96	1.40	1226	1192	2.86	0.24
La	139	89	87	0.35	0.40	20.1	20.6	0.19	0.92	38	38.9	0.98	2.52
Ce	140	160	155	1.29	0.83	19.3	52.3	0.45	0.86	67	67.0	0.17	0.25
Pr	141	18	15.0	0.23	1.53	6.01	6.20	0.1	1.61	7.6	7.83	0.39	4.98
Nd	146	55	50.7	0.52	1.03	25.8	28.9	0.8	2.77	33	32.8	0.23	0.70
Sm	147	7.2	6.65	0.08	1.20	7.72	9.69	0.27	2.79	5.9	5.84	0.10	1.71
Eu	151	1.4	1.42	0.03	2.11	0.09	0.11	0.005	4.55	1.64	1.63	0.01	0.61
Gd	157	4.3	3.79	0.11	2.90	7.1	9.34	0.06	0.64	5	4.84	0.23	4.75
Tb	159	0.48	0.48	0.02	4.17	1.5	1.57	0.05	3.18	0.7	0.67	0.02	2.99
Dy	161	2.4	2.55	0.08	3.14	11.5	11.6	0.46	3.98	3.6	3.79	0.18	4.75
Ho	165	0.4	0.46	0.01	2.17	1.4	2.79	0.03	1.08	0.67	0.74	0.03	4.05
Er	166	0.92	1.08	0.01	0.93	4.95	8.94	0.05	0.56	1.7	1.92	0.09	4.69
Tm	169	0.18	0.16	0.006	3.75	0.7	1.47	0.04	2.72	0.34	0.27	0.01	3.70
Yb	172	0.8	0.70	0.01	1.43	7.34	11.4	0.33	2.88	1.72	1.71	0.06	3.51
Lu	175	0.11	0.10	0.003	3.00	1.22	1.96	0.06	3.06	0.27	0.27	0.01	3.70
Hf	178	7.9	8.11	0.07	0.86	5.36	5.81	0.17	2.93	5.1	4.64	0.07	1.51
Ta	181	0.88	0.77	0.01	1.30	1.9	2.09	0.06	2.87	0.9	0.93	0.02	2.15
Pb	208	30	29.6	0.70	2.36	32.8	30.9	0.93	3.01	36	38.9	0.21	0.54
Th	232	24.7	23.0	0.35	1.52	29.7	29.6	0.98	3.32	6.5	6.75	0.21	3.11
U	238	2.07	1.84	0.04	2.17	12.5	12.2	0.55	4.53	1.92	1.99	0.04	2.01

G-2 and AGV-1 are granite and andesite from USGS, respectively. JG-2 is granite from JGS. *n*=Number of analysis; Rec=recommended values (Goveindaraju, 1994); Obt=obtained values (this study); Std=standard deviation; RSD=relative standard deviation.

## References

- Ames, L., Tilton, G.R., Zhou, G., 1993. Timing of collision of the Sino–Korea and Yangtze cratons: U–Pb dating of coesite-bearing eclogites. *Geology* 21, 339–342.
- Ames, L., Zhou, G., Xiong, B., 1996. Geochronology and geochemistry of ultrahigh-pressure metamorphism with implications for collision of the Sino–Korea Cratons, Central China. *Tectonics* 15, 472–489.
- Anderson, T.B., 1998. Extensional tectonics in the Caledonides of southern Norway, an overview. *Tectonophysics* 98, 333–351.
- Arndt, N.T., Goldstein, S.L., 1987. Use and abuse of crust-formation ages. *Geology* 15, 893–895.
- Bark, F., Arth, J.G., 1976. Generation of trondhjemitic–tonalitic liquids and Archean bimodal trondhemitic–basalt suit. *Geology* 4, 596–600.
- Chavagnac, V., Jahn, B.-M., 1996. Coesite-bearing eclogites from the Bixiling Complex, Dabie Mountains, China: Sm–Nd ages, geochemical characteristics and tectonic implications. *Chem. Geol.* 133, 29–51.
- Chen, J., Jahn, B.-M., 1998. Crustal evolution of southeastern China: Nd and Sr isotopic evidence. *Tectonophysics* 284, 101–133.
- Chen, J., Xie, Z., Liu, S., Li, X., Foland, K.A., 1995. Determination of cooling ages of the Dabie orogenic belt by  $^{40}\text{Ar}/^{39}\text{Ar}$  and fission track dating. *Sci. China, Ser. B* 25, 1086–1092.
- Cong, B., Wang, Q., Zhai, M., 1996. Ultrahigh-Pressure Metamorphic Rocks in the Dabie–Sulu Region of China. Science Press, Beijing, pp. 1–285.
- Cong, B., Wang, Q., Zhai, M., 1999. New data regarding hotly debated topics concerning UHP metamorphism of the Dabie–Sulu belt, east-central China. *Int. Geol. Rev.* 41, 827–835.
- Downes, H., Duthou, J.L., 1988. Isotopic and trace element arguments for the lower crustal origin of Hercynian granitoids and pre-Hercynian orthogneisses, Massif Central (France). *Chem. Geol.* 68, 291–308.
- Farmer, G.L., 1992. Magmas as tracer of lower crustal composition: an isotopic approach. In: Foutain, D.M., Arculus, R., Kay, R.W. (Eds.), *Continental Lower Crust Development in Geotectonics*. Elsevier, Amsterdam, pp. 363–390.
- Faure, M., Lin, W., Shu, L., Sun, Y., Scharer, U., 1999. Tectonics of the Dabieshan (East China) and possible exhumation mechanism of ultrahigh-pressure rocks. *Terra Nova* 11, 251–258.
- Gao, S., Ling, W., Qiu, Y., Lian, Z., Hartmann, G., Simon, K., 1999. Contrasting geochemical and Sm–Nd isotopic compositions of Archean metasediments from the Kongling high-grade terrain of the Yangtze craton: evidence for cratonic evolution and redistribution of REE during crustal anatexis. *Geochim. Cosmochim. Acta* 63, 2071–2088.
- Goveindaraju, G., 1994. Compilation of working values and sample description for 383 geostandards. *Geostand. Newsl.* 18, 1–158 (special issue).
- Hacker, B.R., Wang, X., Eide, E.A., 1996. The Qinling–Dabie ultrahigh-pressure collisional orogen. In: Yin, A., Harrison, T.M. (Eds.), *The Tectonics of Asia*. Cambridge Univ. Press, Cambridge, pp. 345–370.
- Hacker, B.R., Ratschbacher, L., Webb, L.E., Ireland, T.R., Walker, D., Dong, S., 1998. U/Pb zircon ages constrain the architecture of the ultrahigh-pressure Qinling–Dabie orogen, China. *Earth Planet. Sci. Lett.* 161, 215–230.
- Hacker, B.R., Ratschbacher, L., Webb, L.E., Ireland, T.R., Calvert, A., Dong, S., Wenk, H.-R., Chateigner, D., 2000. Exhumation of ultrahigh-pressure continental crust in east-central China: Late Triassic–Early Jurassic tectonic unroofing. *J. Geophys. Res.* 105, 13339–13364.
- Jahn, B.-M., 1998. Geochemical and isotopic characteristics of UHP eclogites and ultramafic rocks of the Dabie orogen: implication for continental subduction and collisional tectonic. In: Hacker, B.R., Liou, J.G. (Eds.), *When Continents Collide: Geodynamics of Ultrahigh Pressure Rocks*. Kluwer Academic Publishing, Netherlands, pp. 203–239.
- Kern, H., Gao, S., Jin, Z., Popp, T., Jin, S., 1999. Petrophysical studies on rocks from the Dabie ultrahigh-pressure (UHP) belt, Central China: implications for the composition and delamination of the lower crust. *Tectonophysics* 301, 191–215.
- Li, S., Wang, T., 1991. Geochemistry of Granitoids in the Tongbaishan–Dabieshan, Central China. China Univ. of Geosciences Press, Wuhan, pp. 1–208 (in Chinese, with English abstract).
- Li, S., Xiao, Y., Liu, D., Chen, Y., Ge, N., Zhang, Z., Sun, S., Cong, B., Zhang, R., Hart, S.R., Wang, S., 1993. Collision of the North China and Yangtze blocks and formation of coesite-bearing eclogites: timing and processes. *Chem. Geol.* 109, 89–111.
- Li, S., Jagoutz, E., Chen, Y., Li, Q., 2000. Sm–Nd and Rb–Sr isotopic chronology and cooling history of ultrahigh pressure metamorphic rocks and their country rocks at Shuanghe in the Dabie Mountains, Central China. *Geochim. Cosmochim. Acta* 64, 1077–1093.
- Liou, J.G., Zhang, R., Eide, E.A., 1996. Metamorphism and tectonics of high-pressure and ultrahigh pressure belts in Dabie–Sulu regions, eastern-central China. In: Yin, A., Harrison, T.M. (Eds.), *The Tectonic Evolution of Asia*. Cambridge Univ. Press, Cambridge, UK, pp. 300–343.
- Liou, J.G., Zhang, R., Jahn, B.-M., 1997. Petrology, geochemistry and isotope data on an ultrahigh pressure jadeite quartzite from Shuanghe, Dabie Mountains, east-central China. *Lithos* 41, 59–78.
- Ma, C., Li, Z., Ehlers, C., Yang, K., Wang, R., 1998. A post-collisional magmatic plumbing system: Mesozoic granitoid plutons from the Dabieshan high-pressure and ultrahigh-pressure metamorphic zone, east-central China. *Lithos* 45, 431–456.
- Ma, C., Ehlers, C., Xu, C., Li, Z., Yang, K., 2000. The roots of the Dabieshan ultrahigh-pressure metamorphic terrane: constraints from geochemistry and Nd–Sr isotope systematics. *Precambrian Res.* 102, 279–301.
- Milisenda, C.C., Liew, T.C., Hofmann, A.W., Kohler, H., 1994. Nd isotopic mapping of the Sri Lanka basement: update and additional constraints from Sr isotopes. *Precambrian Res.* 66, 95–110.
- Okay, A.I., Xu, S., Sengor, A.M.C., 1989. Coesite from the Dabie Shan eclogites, Central China. *Eur. J. Mineral.* 1, 595–598.
- Okay, A.I., Sengor, A.M.C., Satm, M., 1993. Tectonics of an ultrahigh-pressure metamorphic terrane, the Dabie Shan/Tongbai Shan region, China. *Tectonics* 12, 1320–1334.
- Pinarelli, L., Boriani, A., Del Moro, A., 1993. The Pb isotopic systematics during crystal contamination of subcrustal magma:

- the Hercynian magmatism in the Serie dei Laghi (Southern Alps), Italy. *Lithos* 31, 51–56.
- Qiu, Y., Gao, S., McNaughton, N.J., Groves, D.I., Ling, W.L., 2000. SHRIMP U–Pb zircon and Nd isotopic evidence for >3.0 Ga continental crust in the Yangtze craton, South China. *Geology* 28, 11–14.
- Ratschbacher, L., Hacker, B.R., Webb, L.E., McWilliams, M.O., Ireland, T.R., Dong, S., Calvert, A., Chateigner, D., Wenk, H.R., 2000. Exhumation of ultrahigh-pressure continental crust in east-central China: Cretaceous and Cenozoic unroofing and the Tan–Lu fault. *J. Geophys. Res.* 105, 13303–13338.
- RGS-Anhui, 1987. Regional Geology of Anhui Province Geological Publishing House, Beijing (in Chinese, with English abstract).
- Rowley, D.B., Xue, F., Tucker, R.D., Peng, Z., Baker, J., Davis, A., 1997. Ages of ultrahigh pressure metamorphism and protolith orthogneisses from the eastern Dabie Shan: U/Pb zircon geochronology. *Earth Planet. Sci. Lett.* 151, 191–203.
- Suo, S., Zhong, Z., You, Z., 1999. Location of Triassic tectonic suture between collided Sino–Korean and Yangtze cratons in Dabie–Sulu region, China. *J. China Univ. Geosci.* 10, 281–286.
- Suo, S., Zhong, Z., You, Z., 2000. Extensional deformation of post ultrahigh-pressure metamorphism and exhumation process of ultrahigh-pressure metamorphic rocks in the Dabie massif, China. *Sci. China, Ser. D* 43, 225–236.
- Taylor, S.R., McLennan, S.M., 1985. *The Continental Crust: Its Composition and Evolution*. Blackwell, Oxford, 132 pp.
- Tsai, C.H., Liou, J.G., 2000. Eclogite-facies relics and inferred ultrahigh-pressure metamorphism in the North Dabie Complex, central-eastern China. *Am. Mineral.* 85, 1–8.
- Wang, Q., Cong, B., 1996. Tectonic implication of UHP rocks from the Dabie Mountains. *Sci. China, Ser. D* 39, 311–318.
- Wang, X., Liou, J.G., 1991. Regional ultrahigh-pressure coesite-bearing eclogitic terrane in Central China: evidence from country rocks, gneiss, marble and metapelite. *Geology* 19, 933–936.
- Wang, X., Liou, J.G., Mao, H.K., 1989. Coesite-bearing eclogites from the Dabie Mountains in Central China. *Geology* 17, 1085–1088.
- Wang, C., Zeng, R., Mooney, W.D., Hacker, B.R., 2000. A crustal model of the ultrahigh-pressure Dabie Shan orogenic belt, China, derived from deep seismic refraction profiling. *J. Geophys. Res.* 105, 10857–10869.
- Wei, C., Shun, Z., Zhang, L., 1997. Determination of eclogite in northern Dabieshan and its geological significance. *Chin. Sci. Bull.* 42, 1832–1836.
- White, A.J.R., Chappell, B.W., 1977. Ultrametamorphism and granulite genesis. *Tectonophysics* 43, 7–22.
- Xie, Z., Wang, Z., Zheng, Y., Chen, J., Zhang, X., 2001. The mineral O isotopic equilibrium of Zhubuyuan and gneiss in the North Dabie Mountains and the Rb–Sr geochronologic affection. *Geochemica* 30, 95–101 (in Chinese, with English abstract).
- Xu, Z., 1987. *Etude Tectonique et microtectonique de la Chine Paléozoïque et Triasique des qintings (Chine)*. Thesis de doctorate, Uni Sci Tec Languedoc, Montpellier.
- Xu, S., Okay, A.I., Ji, S., Sengor, A.M.C., Su, W., Liu, Y., 1992. Diamond from the Dabie Shan metamorphic rocks and its implication for tectonic setting. *Science* 256, 80–82.
- Xu, S., Liu, Y., Jiang, L., Su, W., 1994. Tectonic Regime and Evolution of Dabie Mountains. Science Press, Beijing, pp. 1–235 (in Chinese, with English abstract).
- Xu, S., Su, W., Liu, Y., Jian, L., Wu, W., 1999. Finding of eclogite in northern Dabieshan and its petrographic characteristics. *Chin. Sci. Bull.* 44, 1452–1456.
- Xue, F., David, B., Rowley, D.B., Tucker, R.D., Peng, Z.X., 1997. U–Pb zircon ages of granitoid rocks in the North Dabie complex, eastern Dabie Shan, China. *J. Geol.* 105, 744–753.
- Ye, K., Cong, B., Ye, D., 2000. The possible subduction of continental material to depths greater than 200 km. *Nature* 407, 734–736.
- You, Z., Han, Y., Yang, W., Zhang, Z., Wei, B., Liu, Y., Jiang, L., 1996. *The High-Pressure and Ultrahigh-Pressure Metamorphic Belt in the East Qinling and Dabie Mountains, China*. China Univ. of Geosciences Press, Wuhan, pp. 1–150 (in Chinese with English abstract).
- Zartman, R.E., Doe, B.R., 1981. Plumbotectonics — the model. *Tectonophysics* 75, 135–162.
- Zhai, M., Cong, B., 1996. Petrotectonics of Sulu–Dabie metamorphic belt, central and east China. *Sci. China, Ser. D* 39, 319–328.
- Zhang, L., 1995. *Block-Geology of Eastern Asia Lithosphere — Isotope Geochemistry and Dynamics of Upper Mantle, Basement and Granite*. Chinese Science Press, Beijing, pp. 1–252.
- Zhang, H., Zhang, B., Zhao, Z., Luo, T., 1996. Continental crust subduction and collision along Shangdan tectonic belt of east Qinling: evidence from Pb, Nd and Sr isotopes of granulites. *Sci. China, Ser. D* 39, 273–282.
- Zhang, H., Gao, S., Zhang, B., 1997. Pb isotopes of granulites suggest Devonian accretion of Yangtze (South China) craton to North China craton. *Geology* 25, 1015–1018.
- Zheng, X., Jin, C., Zhai, M., Shi, Y., 2000. Approach to the source of the gray gneisses in North Dabie terrain: Sm–Nd isochron age and isotope composition. *Acta Petrol. Sin.* 16, 194–198 (in Chinese with English abstract).
- Zhou, T., Chen, J., Li, X., Foland, K.A., 1992.  $^{40}\text{Ar}/^{39}\text{Ar}$  isotopic dating of intrusions from Huoshan–Shucheng syenite zone. *Anhui Geol.* 2, 4–11 (in Chinese with English abstract).